J Fluoresc (2015) 25:1449–1459
DOI 10.1007/s10895-015-1635-9

ORIGINAL ARTICLE

A new Dual-Channel Chemosensor Based on Chemodosimeter Approach for Detecting Cyanide in Aqueous Solution: a Combination of Experimental and Theoretical Studies

Jae Jun Lee[1] · **Sun Young Lee**[1] · **Kwon Hee Bok**[1] · **Cheal Kim**[1]

Received: 30 June 2015 / Accepted: 26 July 2015 / Published online: 6 August 2015

Abstract A new colorimetric and fluorescent receptor **1** for the detection of CN^- has been simply developed. Receptor **1** showed selectively colorimetric and fluorometric responses to CN^- in a near-perfect aqueous solution, respectively. This sensor displayed an obvious color change from yellow to colorless upon selective binding with CN^-. In addition, it could function as an "OFF-ON type" fluorescent response through a nucleophilic addition mechanism. The binding mode of receptor **1** with CN^- was proposed to be 1:1, based on Job plot, ^1H NMR titration and ESI-mass spectrometry analysis. Moreover, the sensing mechanism for CN^- was theoretically supported by DFT and TD-DFT calculations.

Keywords Cyanide · Colorimetric · Fluorescent · DFT calculations

Introduction

Development of chemical sensors for anions is of great interest due to their important roles in biological, industrial and environmental process [1–5]. Among the various anions, cyanide is extensively utilized in many fields such as gold mining, electroplating, metallurgy, synthetic fibers and resins industry. Therefore, the wide use of cyanide is inevitable, and many industries produce nearly 140,000 tons of cyanide per year worldwide [6–10]. On the other hand, cyanide is known to be damaging anion causing poison in biology and environment. It has propensity to bind to the iron in cytochrome c oxidase, interfering with electron transport and resulting in hypoxia [11–15]. Thus, there is a strong demand for an efficient sensing method to monitor cyanide.

A variety of sensors for cyanide have been developed via various kinds of sensing methods, such as atomic absorption, electrochemical methods and mass spectroscopy [16–19]. The major limitation of these methods is the use of time-consuming procedures that involve the use of sophisticated instrumentation. However, colorimetric and fluorescence approaches could be used to overcome the limitation. The colorimetric approach allows naked-eye detection of the color change without resorting to the use of expensive instruments [20–22]. In addition, the fluorescence approach can detect interesting analytes with fast response, convenient procedures, and high sensitivity [23–36]. For this reasons, scientists have devoted many efforts to design colorimetric and fluorescent chemosensors for monitoring cyanide [25–47].

Chemodosimeters are molecular probes used to achieve the recognition of analyte with the irreversible process. They have been intensively studied in the anion sensing area, because they have advantage of high selectivity by the minimized interference of other anions [48–55]. Nevertheless, they still suffer from the high detection limit and decreased reaction rate in aqueous solution. To overcome the challenges, therefore, we developed a new colorimetric and fluorescent sensor, which has an imine moiety acting as a nucleophilic acceptor.

Herein, we report a new triazole-based chemosensor **1**, which was synthesized in one step by condensation reaction of 3,5-diamino-1,2,4-triazole and 2-hydroxy-1-naphthalehyde (Scheme 1). Chemosensor **1** detected cyanide by both color

Electronic supplementary material The online version of this article (doi:10.1007/s10895-015-1635-9) contains supplementary material, which is available to authorized users.

✉ Cheal Kim
chealkim@snut.ac.kr

[1] Department of Fine Chemistry and Department of Interdisciplinary Bio IT Materials, Seoul National University of Science and Technology, Seoul 139-743, Korea

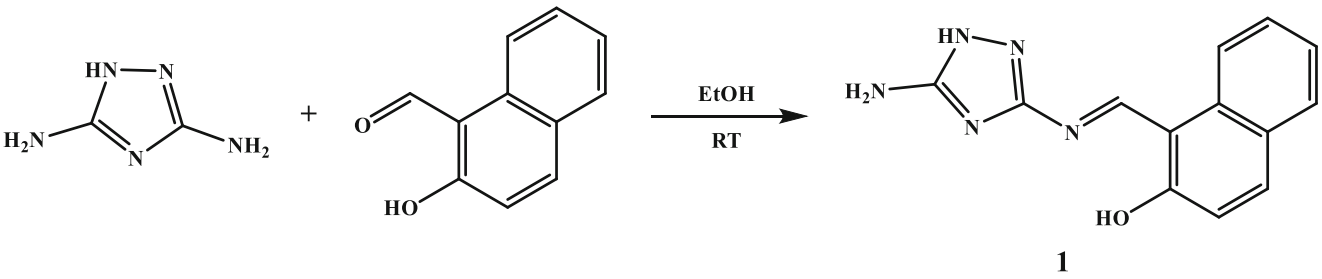

Scheme 1 Synthetic procedure of chemosensor **1**

change from yellow to colorless and fluorescence enhancement in a near-perfect aqueous solution. A nucleophilic addition mechanism for sensing of CN^- was proposed, which was supported by the DFT/DT-DFT calculation method.

Experiments

Reagents and Instrument

All reagents were commercially obtained from Sigma-Aldrich (St. Louis, Mo, USA) and used without further purification. Anhydrous ethanol was prepared by the simple distillation from $MgSO_4$. Fluorescence measurements were performed on a Perkin Elmer model LS45 fluorescence spectrometer. The ^1H NMR measurements were performed on a Varian 400 MHz spectrometer and 100 MHz spectrometer, respectively and the chemical shifts were recorded in ppm. Electrospray ionization mass spectra (ESI-MS) were collected on a thermo Finnigan (San Jose, CA, USA) LCQTM Advantage MAX quadrupole Ion trap instrument. Elemental analysis for carbon, nitrogen and hydrogen was carried out by using Flash EA 1112 Elemental analyzer (thermo) in Organic Chemistry Research Center of Sogang University, Korea.

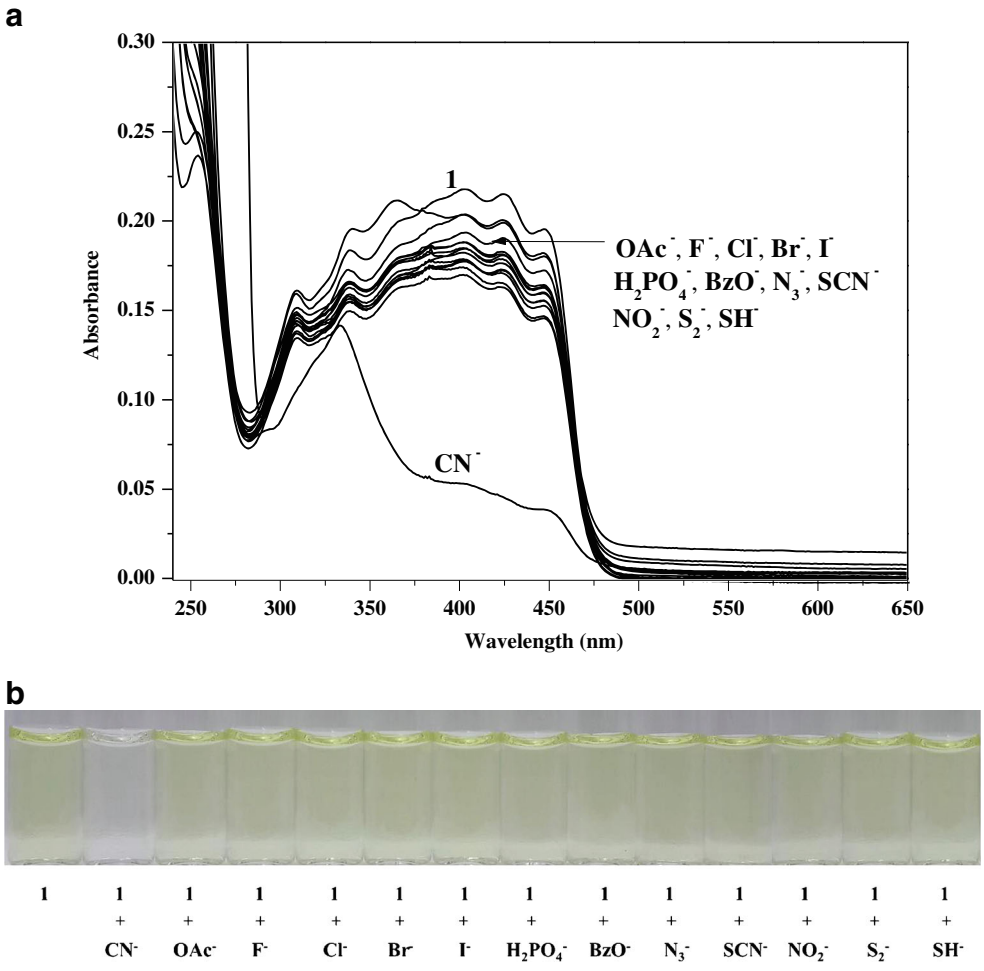

Fig. 1 **a** Absorption spectral changes of **1** (20 μM) in the presence of 12 equiv. of different anions in bis-tris buffer (10 mM bis-tris, pH=7.0). **b** The color changes of **1** (20 μM) upon addition of various anions (12 equiv.) in bis-tris buffer (10 mM bis-tris, pH=7.0)

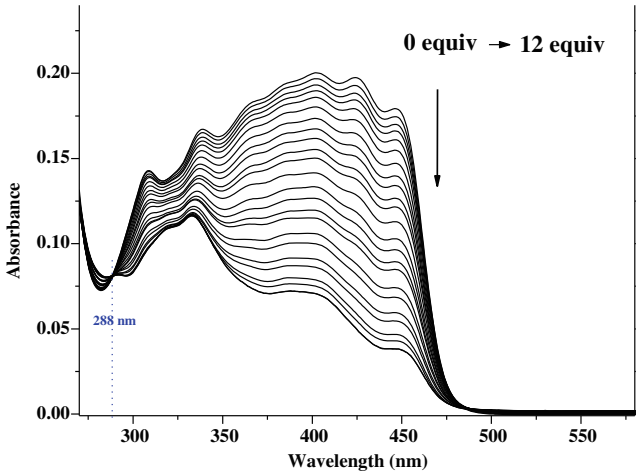

Fig. 2 Absorption spectral changes of **1** (20 μM) in the presence of different concentrations of CN^- (from 0 to 12 equiv.) at room temperature

Absorption spectra were recorded at 25 °C using the Perkin Elmer model Lambda 25 UV/vis spectrometer. All electronic figures were created by Origin 8.0.

Synthesis of 1

3,5-Diamino-1,2,4-triazole (151.7 mg, 1.5 mmol) in ethanol (10 mL) was added to a solution containing 2-hydroxy-1-naphthalehyde (298.7 mg, 1.7 mmol) in ethanol (10 mL). The reaction mixture was stirred for 1 d, until the yellow precipitate appeared. The precipitate was filtered and washed with ether (10 mL×2) and ethanol (10 mL). The yield was 69 % (262.1 mg). ^{1}H NMR (400 MHz, DMSO-d_6, ppm) δ 12.13 (s, 1H), 9.84 (s, 1H), 8.21 (d, J=8.7 Hz, 1H), 8.00 (d, J=9.2 Hz, 1H), 7.87 (d, J=8.1 Hz, 1H), 7.60 (t, J=7.7 Hz, 1H), 7.41 (t, J=7.5 Hz, 1H), 7.13 (d, J=9.1 Hz, 1H), 6.30 (s, 2H); ^{13}C NMR (100 MHz, DMSO-d_6, ppm): 166.36 (1C), 160.37 (1C), 157.71 (1C), 157.30 (1C), 136.61 (1C), 133.02 (1C), 129.66 (1C), 128.89 (1C), 127.64 (1C), 124.18 (1C), 120.89 (1C), 120.03 (1C), 108.95 (1C). LRMS (ESI): m/z calcd for $C_{13}H_{10}N_5O$: 252.089 ([M-H$^+$]); found, 252.267. Anal. calcd for $C_{13}H_{11}N_5O$ (249.273): C, 61.65; H, 4.38; N, 27.65; found: C, 61.75; H, 4.39; N, 27.93.

UV–vis Measurements of Receptor 1 with CN^-

Receptor **1** (0.4 mg, 0.0015 mmol) was dissolved in DMSO (0.5 mL) and 20 μL of the receptor **1** (3 mM) were diluted to 2.980 mL bis-tris buffer to make the final concentration of 20 μM. Tetraethylammonium cyanide (TEACN, 49.3 mg, 0.3 mmol) was dissolved in bis-tris buffer (1 mL). 0.2-4.2 μL of the CN^- solution (300 mM) were transferred to each receptor solution (20 μM) prepared above. After mixing them for a few seconds, UV–vis absorption spectra were taken at room temperature.

Fluorescence Measurements of Receptor 1 with CN^-

Receptor **1** (0.4 mg, 0.0015 mmol) was dissolved in DMSO (0.5 mL) and 20 μL of the receptor **1** (3 mM) were diluted to 2.980 mL bis-tris buffer to make the final concentration of 20 μM. TEACN (49.3 mg, 0.3 mmol) was dissolved in bis-tris buffer (1 mL). 0.2–3.2 μL of the CN^- solution (300 mM) were transferred to each receptor solution (20 μM) prepared above. After mixing them for a few seconds, fluorescent spectra were taken at room temperature.

Job Plot Measurement

Receptor **1** (12.7 mg, 0.05 mmol) was dissolved in DMSO (5 mL). 12, 10.8, 9.6, 8.4, 7.2, 6.0, 4.8, 3.6, 2.4, 1.2 and 0 μL of receptor **1** solution were taken and transferred to vials. Each vial was diluted with bis-tris buffer to make a total volume of 2.988 mL. TEACN (8.2 mg, 0.05 mmol) was dissolved in bis-tris buffer (5 mL). 0, 1.2, 2.4, 3.6, 4.8, 6.0, 7.2, 8.4, 9.6, 10.8, and 12 μL of the TEACN solution were added to each diluted receptor **1** solution. Each vial had a total volume of 3 mL. After shaking the vials for a few seconds, UV–vis spectra were taken at room temperature.

Competition with Other Anions

Receptor **1** (0.4 mg, 0.0015 mmol) was dissolved in DMSO (0.5 mL) and 20 μL of the receptor **1** (3 mM) were diluted to 2.980 mL bis-tris buffer to make the final concentration of

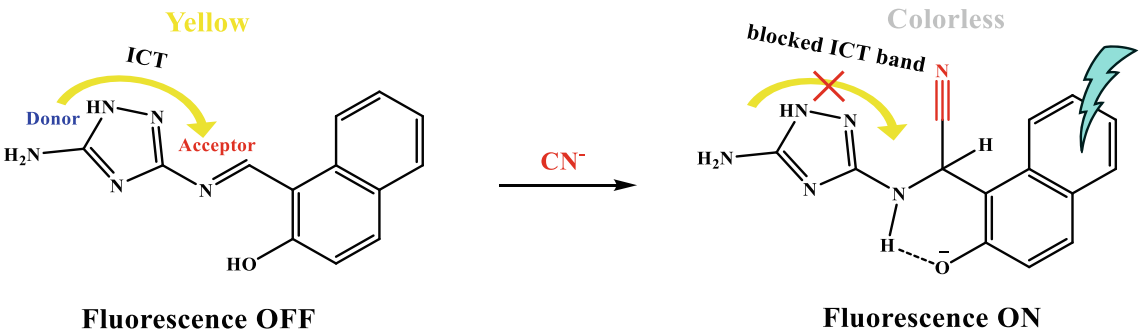

Scheme 2 The proposed colorimetric and fluorescent sensing mechanism of **1** for CN^-

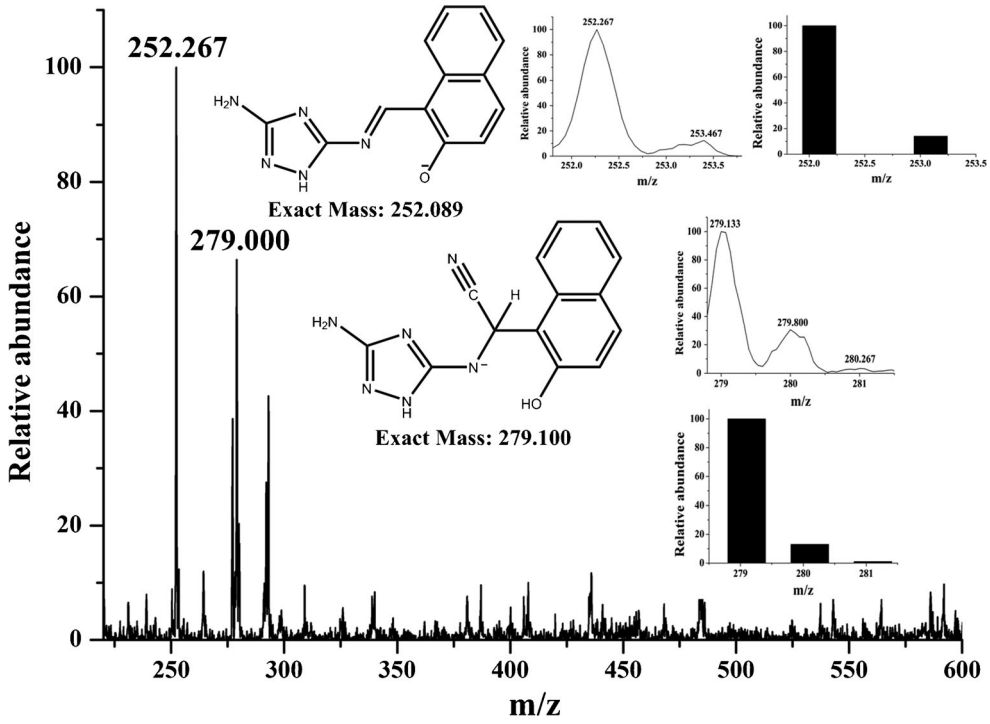

Fig. 3 Negative-ion electrospray ionization mass spectrum of **1** (20 μM) upon addition of TEACN (12 equiv.)

20 μM. Tetraethylammonium (TEA) salts (F^-, Cl^-, Br^-, I^-, 0.3 mmol) or tetrabuthylammonium (TBA) salts (OAc^- $H_2PO_4^-$, N_3^-, SCN^-, BzO^-, 0.3 mmol) or Na salts (NO_2^-, S_2^-, SH^-, 0.3 mmol) were separately dissolved in bis-tris buffer (1 mL). 3.2 μL of each anion solution (300 mM) were taken and added into 2.968 mL of each **1** solution (20 μM) prepared

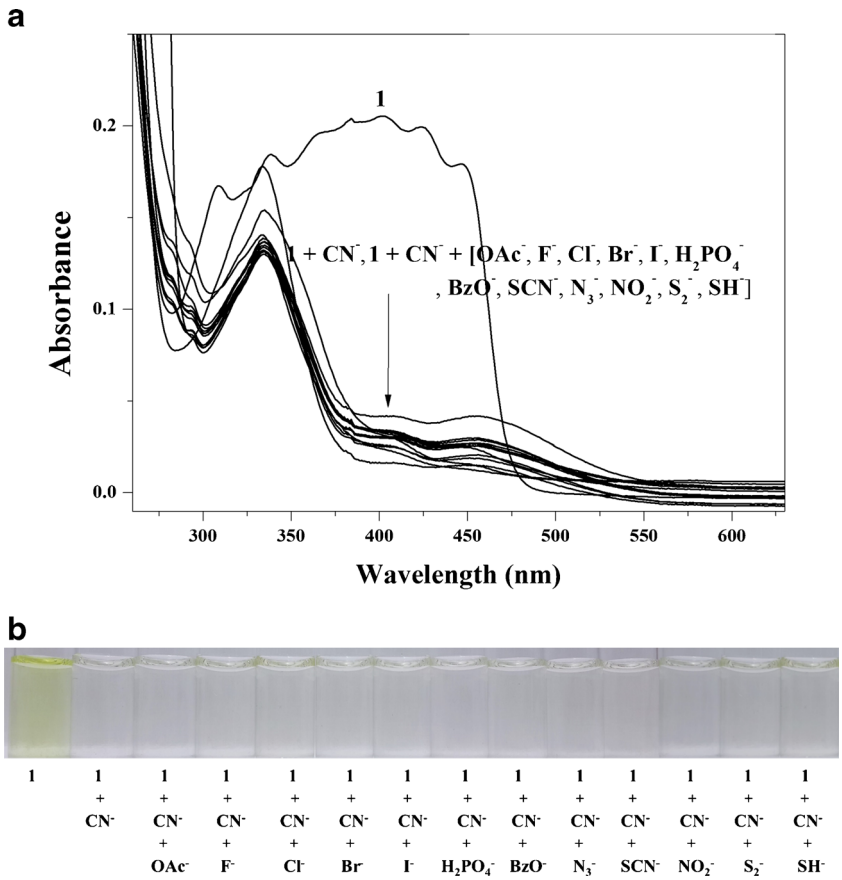

Fig. 4 **a** Absorption spectral changes of **1** (20 μM) upon addition of cyanide (12 equiv.) in the absence and presence of 12 equiv. of various anions in bis-tris buffer (10 mM bis-tris, pH=7.0). **b** The color changes of **1** (20 μM) upon addition of cyanide (12 equiv.) in the absence and presence of 12 equiv. of various anions in bis-tris buffer (10 mM bis-tris, pH=7.0)

above to make 16 equiv. Then, 3.2 μL of the TEACN solution (300 mM) were added into the mixed solution of each anion and **1** to make 16 equiv. After mixing them for a few seconds, UV–vis and fluorescence spectra were taken at room temperature, respectively.

^{1}H NMR Titration

For ^{1}H NMR titrations of receptor **1** with CN^-, five NMR tubes of receptor **1** (2.5 mg, 0.01 mmol) dissolved in DMSO-d_6/CD_3OD (v/v=6:4) were prepared and then five different concentrations (0, 0.015, 0.03, 0.09 and 0.12 mmol) of TEACN dissolved in CD_3OD were added to each solution of receptor **1**. After shaking them for a minute, ^{1}H NMR spectra were taken at room temperature.

Calculation Methods

All theoretical calculations were performed by DFT/TD-DFT method with the hybrid exchange-correlation functional B3LYP [56, 57] applying the 6-31G**[58, 59] basis set without any symmetry restrictions in the gas phase. The energy-minimized structure of **1** was obtained in various geometric forms. On the basis of the optimized ground (S_0) structure of

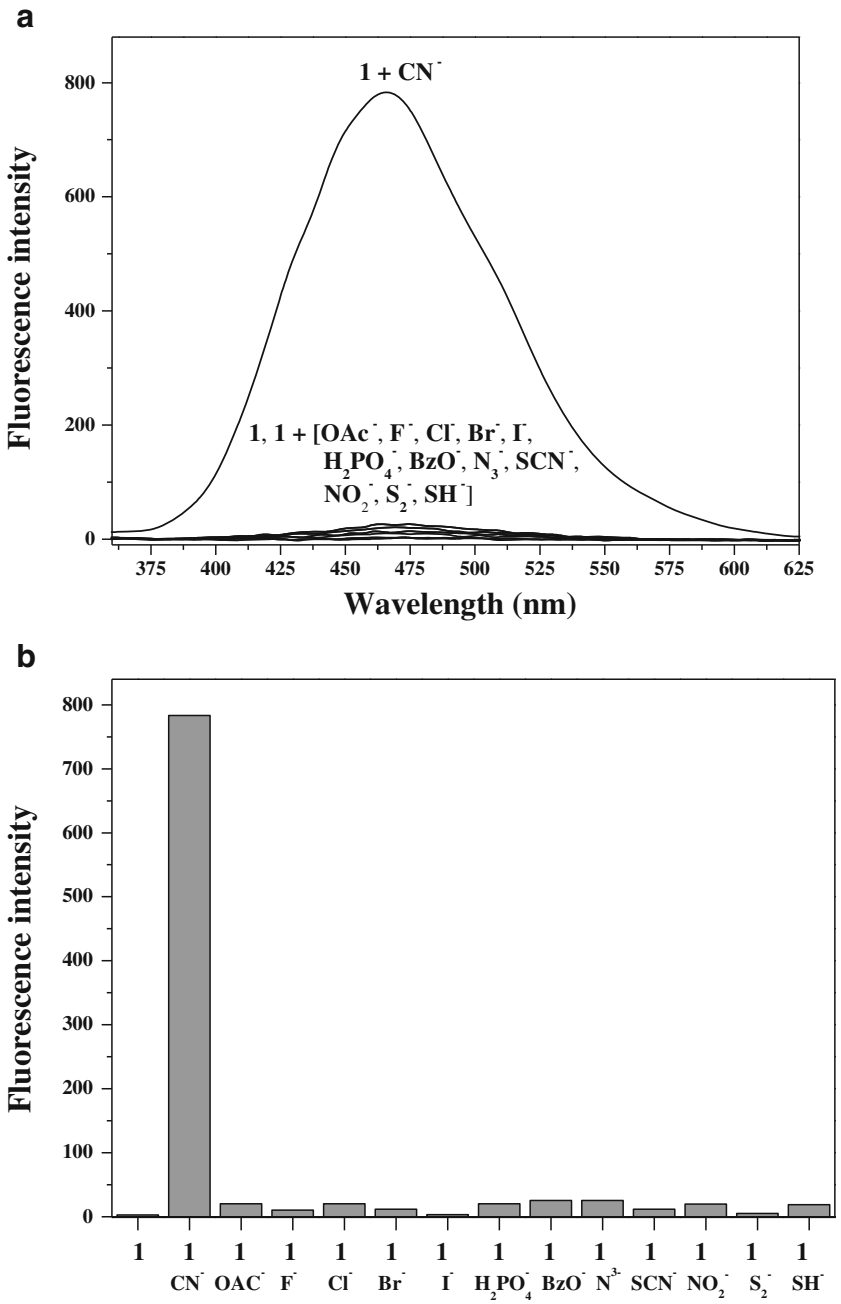

Fig. 5 **a** Fluorescence spectra of **1** (20 μM, λ_{ex}=335 nm) upon addition of various anions (16 equiv.) in bis-tris buffer (10 mM bis-tris, pH=7.0). **b** Bar graph representing the change of the relative emission intensity of **1** (20 μM) at 466 nm upon treatment with various anions

1, the optimized structures of **1**-CN^- were also obtained. In vibrational frequency calculations, there was no imaginary frequency for the optimized geometries of **1** and **1**-CN^-, suggesting that these geometries represented local minima. For all calculations, the solvent effect of water was considered by using the Cossi and Barone's CPCM (conductor-like polarizable continuum model) [60, 61]. In order to investigate the transition energies for the optimized structures of **1** and **1**-CN^-, we calculated the lowest 20 singlet-singlet transition using their ground state geometry (S_0) with TD-DFT (B3LYP) method. The GaussSum 2.1 was used to calculate the contribution of molecular orbital in electronic transitions [62]. All the calculations were performed with Gaussian 03 suite [63].

Results and Discussion

Synthesis of 1

The receptor **1** was obtained by coupling 3,5-diamino-1,2,4-triazole and 2-hydroxyl-1-naphthaldehyde with 70 % yield in ethanol (Scheme 1) and analysed by ^{1}H NMR, ^{13}C NMR, ESI-mass spectrometry and elemental analysis.

Colorimetric and Fluorescent Cyanide Sensing

The colorimetric sensing properties of **1** toward CN^- were studied by UV–vis spectrometry (Fig. 1). When various anions (TEA salts: F^-, Cl^-, Br^-, I^-, CN^-; TBA salts: OAc^-, $H_2PO_4^-$, N_3^-, SCN^-, BzO^-; Na salts: NO_2^-, S_2^-, SH^-) in bis-tris buffer solution (10 mM, pH 7.0) were added into the **1** solution, only CN^- showed UV–vis change with a complete decrease of absorption band at 400 nm (Fig. 1a). Consistent with the change in UV–vis spectrum, the solution of **1** resulted in a color change from yellow to colorless with cyanide ion (Fig. 1b). These results proposed that CN^- might attack the imine group of **1** via a nucleophilic addition mechanism, resulting in colorless [38, 64, 65].

To further investigate the binding property of **1** with CN^-, the UV–vis titration experiments were performed (Fig. 2). The absorption spectrum of **1** showed a broad band in a range of 350 to 450 nm, which might be attributed to the transition of intramolecular charge transfer (ICT) band. It is known that chemosensor containing an electron-donating group ($-NH_2$) and an electron-withdrawing group (−C=N-) undergoes ICT from the donor to the acceptor following electronic excitation (Scheme 2) [66–68]. On treatment with CN^- to solution of **1**, the absorption band at 400 nm was gradually attenuated and reached minimum at 12 equiv. of CN^-, and a clear isosbestic point was observed at 288 nm. A noticeable decrease of the absorption band at 400 nm suggested that the transition of ICT might be interrupted by the nucleophilic addition reaction of CN^- to **1** (Scheme 2) [38, 64, 65].

The Job plot [69] referred to a 1:1 stoichiometry between **1** and CN^- (Fig. S1), which was further confirmed by ESI-mass spectrometry analysis (Fig. 3). The negative-ion mass spectrum showed the formation of the **1**-CN^- complex [calcd: 279.100, *m/z*: 279.000 for **1**+CN^-]. Based on the UV–vis titration, Job plot and ESI-mass analysis, we proposed the sensing mechanism of **1** for CN^- as shown in Scheme 2. The detection limit of **1** for CN^- was determined to be 35 μM, based on the 3σ/slope (Fig. S2) [70].

To explore the ability of **1** as a colorimetric chemosensor for CN^-, the competition experiments were conducted in the presence of CN^- mixed with various competing anions (Fig. 4). When **1** was treated with 12 equiv. of CN^- in presence of the same concentration of other anions, all these competing anions showed no obvious interference with naked-eye detection of CN^- by **1**. These results indicated that chemosensor **1** could be a good CN^- sensor over other competing anions in aqueous solution.

For biological application, the pH dependences of **1** in the absence and presence of CN^- were examined at various pH. The decrease of absorbance caused by adding CN^- was observed between 7 and 12 (Fig. S3), which warrants its application for detection of CN^- by **1** under physiological conditions.

Next, to examine the fluorescent properties of **1**, the emission was measured with various anions (TEA salts: F^-, Cl^-, Br^-, I^-, CN^-; TBA salts: OAc^-, $H_2PO_4^-$, N_3^-, SCN^-, BzO^-; Na salts: NO_2^-, S_2^-, SH^-) in bis-tris buffer solution (10 mM, pH 7.0). Receptor **1** alone has a weak fluorescence emission (λ_{max}=466 nm and λ_{ex}=335 nm) (Fig. 5). When 16 equiv. of anions such as CN^-, OAc^-, F^-, Cl^-, Br^-, I^-, $H_2PO_4^-$, N_3^-, SCN^-, BzO^-, NO_2^-, S_2^-, and SH^- were added to the sensor **1**, it was found that the solution of **1** exhibited either no or small increases of the fluorescence. In contrast, the addition of CN^- into **1** showed a remarkable fluorescence enhancement

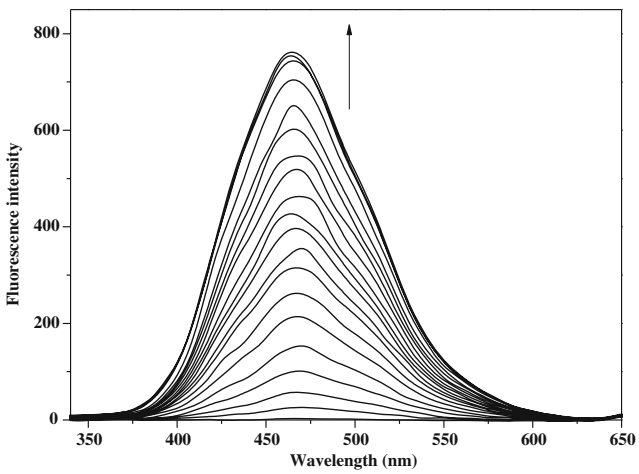

Fig. 6 Fluorescence spectra of **1** (20 μM, λ_{ex}=335 nm) in the presence of increasing different concentration of CN^- (from 0 to 16 equiv.) at room temperature

(390-folds) of emission intensity at 466 nm. These results indicated that sensor **1** could be used as a fluorescence chemosensor for CN^-.

To further investigate the chemosensing properties of **1**, fluorescence titration of the sensor **1** with CN^- ion was performed. As shown in Fig. 6, the emission intensity of **1** at 466 nm gradually increased until the amount of CN^- reached 16 equiv. This observation with the UV–vis titration results, again, suggested that the ICT process was inhibited upon the addition of CN^-, as shown in Scheme 2. That is, the nucleophilic addition of CN^- to the imine group of **1** prevented ICT, and the naphthol group functioned as a fluorophore, which induced the fluorescence enhancement of **1**-CN^-.

To explore the ability of **1** as a fluorescence chemosensor for CN^-, the competition experiments were performed in the presence of CN^- mixed with various anions. When **1** was treated with 16 equiv. of CN^- in the presence of the same concentration of other anions (Fig. 7), other background anions had no obvious interference with the detection of CN^-

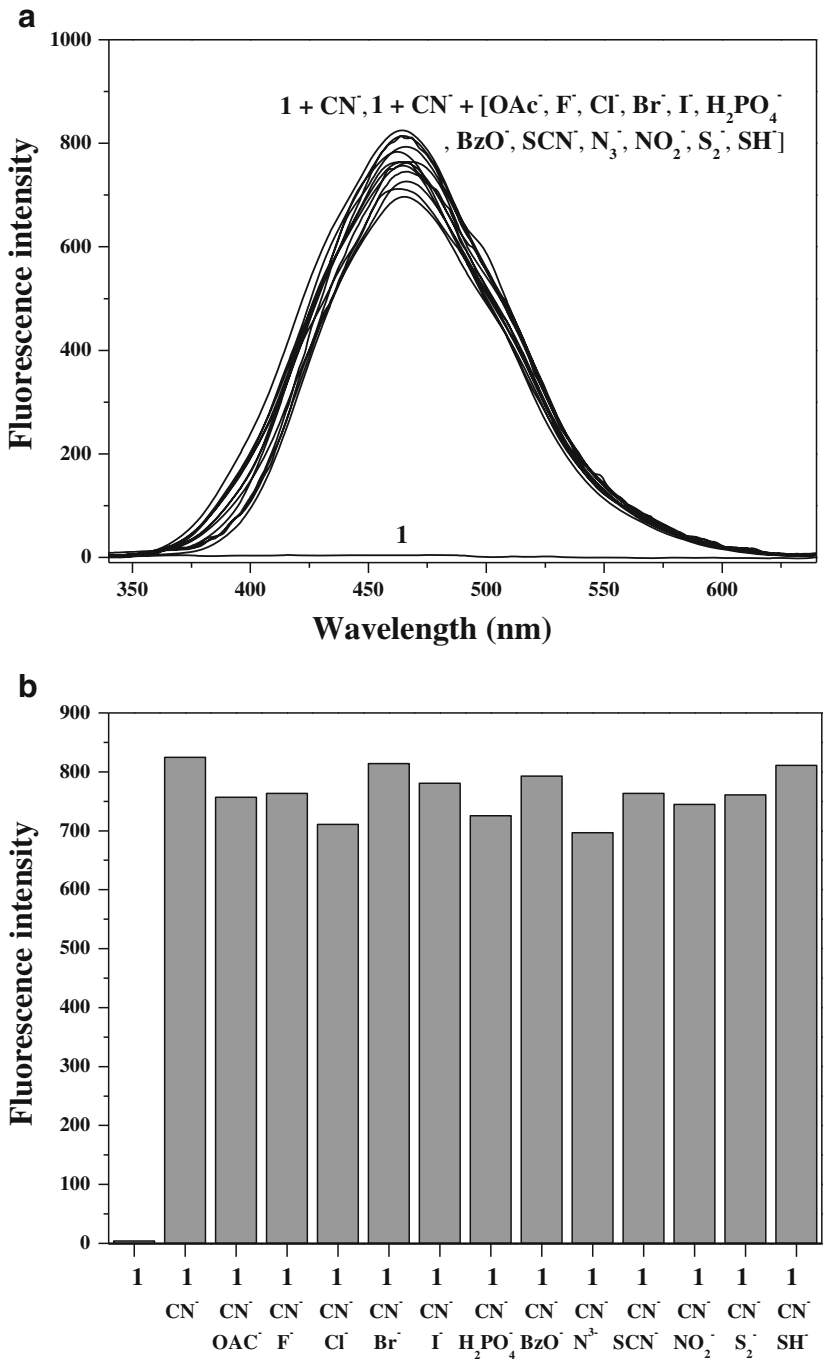

Fig. 7 **a** Fluorescence spectral changes of **1** (20 μM, λ_{ex}= 335 nm) upon addition of cyanide (16 equiv.) in the absence and presence of 16 equiv. of various anions in bis-tris buffer (10 mM bis-tris, pH=7.0). **b** Bar graph representing the fluorescence intensity of **1** (20 μM, λ_{ex}= 335 nm, λ_{em}=466 nm) with cyanide (16 equiv.) in the absence and presence of 16 equiv. of various anions in bis-tris buffer (10 mM bis-tris, pH=7.0)

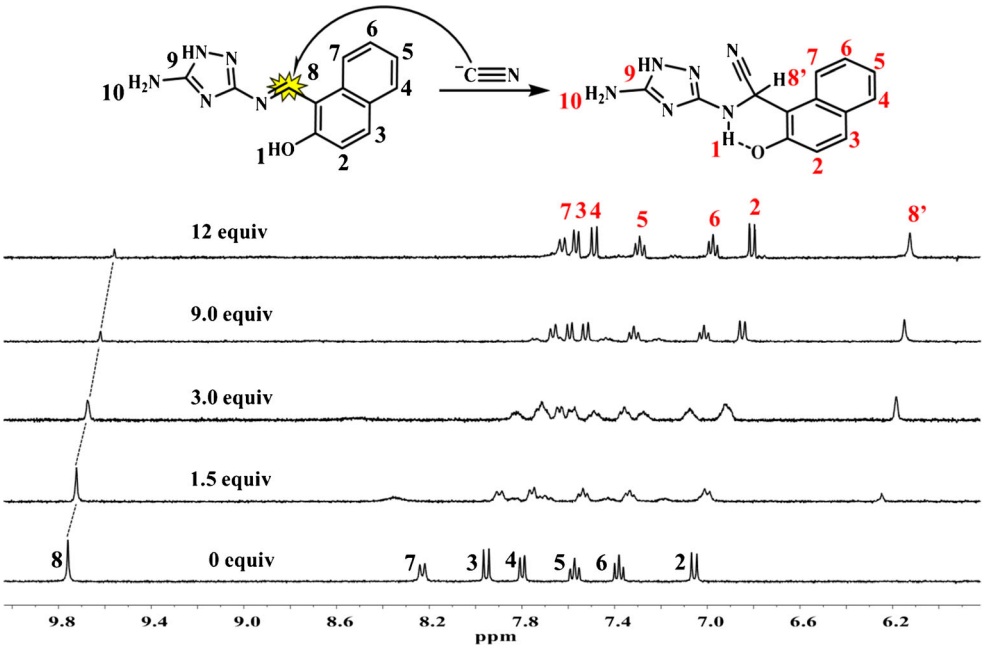

Fig. 8 ^{1}H NMR titration of **1** with CN^{-}

ion. These results indicated that chemosensor **1** could be a good CN^{-} sensor over other competing anions in aqueous solution.

In order to further examine the proposed nucleophilic addition of CN^{-} toward chemosensor **1**, ^{1}H NMR titrations were performed (Fig. 8). Upon addition of 12 equiv. of CN^{-}, the H_8 protons of imine group at 9.8 ppm gradually disappeared and a new $H_{8'}$ proton at 6.1 ppm started to appear. This result strongly suggested that the nucleophilic addition of CN^{-} occurred at the carbon atom of imine group of **1** [64, 65, 71–74]. All the aromatic protons were shifted to upfield, which suggests that the negative charge developed from the nucleophilic addition of CN^{-} to **1** might be delocalized through the whole receptor molecule.

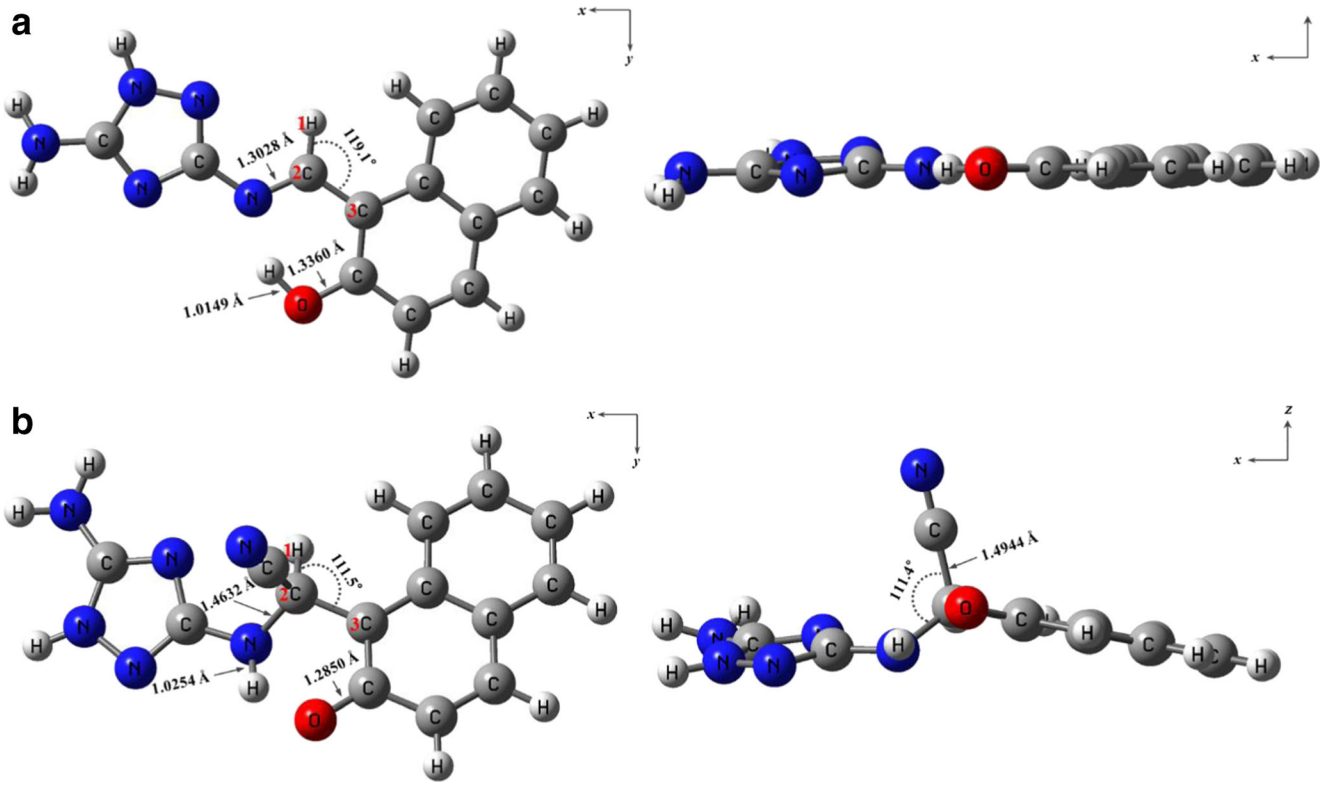

Fig. 9 Energy-minimized structures of (**a**) **1** and (**b**) **1**-CN^{-}

For biological application, the pH dependence of **1** in the absence and presence of CN^- was examined at various pH. The increase of fluorescence intensity caused by adding CN^- was observed between 7 and 10 (Fig. S4), which warrants its application for detection of CN^- by **1** under physiological conditions.

Theoretical Calculations for Sensing Mechanism of CN^-

In parallel to the experimental study, to further get understanding on the electronic structures of **1** and **1**-CN^-, we optimized energy-minimized structures of chemosensor **1** and **1**-CN^- at DFT/B3LYP/6-31G** level. Their energy-minimized structures were shown in Fig. 9, and bond lengths and angles were compared between **1** and **1**-CN^-. In addition, the relationship between orbital hybridisation and conjugation was compared. **1** was close to a sp^2 hybridized imine group (bond angle=119.1° (H1, C2, C3)) and planar conformation, whereas **1**-CN^- was close to a sp^3 hybridized carbon bond (bond angle=111.5° (H1, C2, C3)) and tilted conformation. This structural difference caused a significant change in π-conjugation between **1** and **1**-CN^-, expecting that no ICT was observed in the **1**-CN^- adduct.

To gain an insight into colorimetric and fluorescent sensing mechanism for **1**-CN^-, time-dependent density functional theory (TD-DFT) calculations were performed at the optimized geometries (S_0). In case of **1**, the main molecular orbital (MO) contribution of the first lowest excited state was determined for HOMO→LUMO transition (384.80 nm, Fig. S5). The HOMO was mainly localized in donor parts, i.e., NH_2- and -NH- in triazole moiety, whereas the LUMO was composed of the atoms of the electron-withdrawing imine group (Fig. S5c), which indicated intramolecular charge transfer (ICT) transition from amine to imine group, resulting in the yellow color of **1**. For **1**-CN^-, the main molecular orbital (MO) contribution of the first lowest excited state was also determined for HOMO→LUMO transition (368.70 nm, Fig. S6). The HOMO was mainly localized in π orbitals of the naphthol group, whereas the LUMO was mainly localized in π* orbitals of the naphthol group (Fig. S6c). These results indicated that the nucleophlic addition of cyanide changed the first excited state from ICT to π→π* transition of the naphthol group. Therefore, the colorimetric sensing mechanism could be explained by blocking of the ICT transition by the nucleophilic addition of CN^- at imine carbon. Moreover, the fluorescence sensing mechanism could be explained that π→π* transition of the naphthol group, the most useful transition in fluorescence, acted as a fluorophore.

Conclusion

We have developed an outstanding single chemosensor **1**, based on a naphtholic Schiff base bearing a triazol group, for CN^- through the two different signaling (colorimetric and fluorescent). Chemosensor **1** showed a highly selective colorimetric and fluorescent response to cyanide via a nucleophlic addition mechanism. The detection of CN^- by **1** was found to be free of interference from any other anions in aqueous solution. Moreover, DFT and TD-DFT studies supported the experimental data and the proposed sensing mechanisms. Thus, this sensor exhibits a new method to assay CN^- by two different detection modes.

Acknowledgments Basic Science Research Program through the National Research Foundation of Korea (NRF) (NRF-2014R1A2A1A11051794) are gratefully acknowledged. We thank Nano-Inorganic Laboratory, Department of Nano & Bio chemistry, Kookmin University to access the Gaussian 03 program packages.

References

1. Xu Z, Kim SK, Yoon J (2010) Revisit to imidazolium receptors for the recognition of anions: highlighted research during 2006–2009. Chem Soc Rev 39:1457–1466
2. Martínez-Máñez R, Sansenón F (2003) Fluorogenic and chromogenic chemosensor and reagents for anions. Chem Rev 103:4419–4476
3. Santos-Figueroa LE, Moragues ME, Climent E, Agostini A, Martínez-Máñez R, Sancenón F (2013) Chromogenic and fluorogenic chemosensor and reagents for anions. A comprehensive review of the years 2010–2011. Chem Soc Rev 42:3489–3613
4. Upadhyay KK, Kumar A (2010) Pyrimidine based highly sensitive fluorescent receptor for Al^{3+} showing dual signalling mechanism. Org Biomol Chem 8:4892–4897
5. Wang F, Wang L, Chen X, Yoon J (2014) Recent progress in the development of fluorometric and colorimetric chemosensors for detection of cyanide ions. Chem Soc Rev 43:4312–4324
6. Hachiya H, Ito S, Fushinuki Y, Masadome T, Asano Y, Imato T (1999) Continuous monitoring for cyanide in waste water with a galvanic hydrogen cyanide sensor using a purge system. Talanta 48:997–1004
7. Wiley-VCH (Editors) (1999) Ullmann's Encyclopedia of Industrial Chemistry, 6th edn Wiley-VCH, New York
8. Koenig R (2000) Wildlife deaths are a grim wake-Up call in Eastern Europe. Science 287:1737–1738
9. Young C, Tidwell L, Anderson C (2001) Cyanide: social, industrial, and economic aspects. Mineral, Metals, and Materials Society, Warrendale
10. Sun H, Zhang YY, Si SH, Zhu DR, Fung YS (2005) Piezoelectric quartz crystal (PQC) with photochemically deposited nano-sized Ag particles for determining cyanide at trace levels in water. Sensors Actuators B 108:925–932
11. Way JL (1984) Cyanide intoxication and its mechanism of antagonism. Annu Rev Pharmacol Toxicol 24:451–481
12. Zamecnik J, Tam J (1987) Cyanide in blood by gas chromatography with NP detector and acetonitrile as internal standard. Application on air accident fire victims. Anal Toxicol 11:47–48
13. Levin BC, Rechani PR, Gurman JL, Landron F, Clark HM, Yoklavich MF, Rodriguez JR, Dros L, Mattos de Cabrera F, Kaye SJ (1990) Analysis of carboxyhemoglobin and cyanide in blood from victims of the Dupont Plaza Hotel fire in Puerto Rico. Forensic Sci Int 35:151–168

14. Matsubara K, Akane A, Maeda C, Shiono H (1990) "First pass phenomenon" of inhaled gas in the fire victims. Forensic Sci Int 46:203–208
15. Mayes RW (1991) High cyanide level in a homicide victim burned after death: evidence of post-mortem diffusion. J Forensic Sci Int 36:179–184
16. Haj-Hussein AT, Christian GD, Ruzicka J (1986) Determination of cyanide by atomic absorption using a flow injection conversion method. Anal Chem 56:38–42
17. Taheri A, Noroozifar M, Khorasani-Motlagh M (2009) Investigation of a new electrochemical cyanide sensor based on Ag nanoparticles embedded in a three-dimensional sol–gel. J Electroanal Chem 628:48–54
18. Minakata K, Nozawa H, Gonmori K, Suzuki M, Suzuki O (2009) Determination of cyanide, in urine and gastric content, by electrospray ionization tandem mass spectrometry after direct flow injection of dicyanogold. Anal Chim Acta 651:81–84
19. Løbger LL, Petersen HW, Andersen JET (2008) Analysis of cyanide in blood by headspace-isotope-dilution-GC-MS. Anal Lett 41: 2564–2586
20. Li KB, Zang Y, Wang H, Li J, Chen GR, James TD, He XP, Tian H (2014) Hepatoma-selective imaging of heavy metal ions using a 'clicked' galactosylrhodamine probe. Chem Commun 50:11735–11737
21. Yang L, Li X, Yang J, Qu Y, Hua J (2013) Colorimetric and ratiometric near-infrared fluorescent cyanide chemodosimeter based on phenazine derivatives. Appl Mater Interfaces 5:1317–1326
22. Mashraqui SH, Betkar R, Chandiramani M, Estarellas C (2011) Design of a dual sensing highly selective cyanide chemodosimeter based on pyridinium ring chemistry. New J Chem 35:57–60
23. Na YJ, Park GJ, Jo HY, Lee SA, Kim C (2014) A colorimetric chemosensor based on a Schiff base for highly selective sensing of cyanide in aqueous solution: the influence of solvents. New J Chem 38:5769–5776
24. Yoo J, Kim Y, Kim SJ, Lee CH (2010) Anion-modulated, highly sensitive supramolecular fluorescence chemosensor for C_{70}. Chem Commun 46:5449–5451
25. Sun Y, Liu Y, Guo W (2009) Fluorescent and chromogenic probes bearing salicylaldehyde hydrazone functionality for cyanide detection in aqueous solution. Sensors Actuators B 143:171–176
26. Lee DY, Singh N, Kim MJ, Jang DO (2011) Chromogenic and fluorescent recognition of iodide with a benzimidazole-based tripodal receptor. Org Lett 12:3024–3027
27. Nam SW, Chen X, Lim J, Kim SH, Kim ST, Cho YH, Yoon J, Park S (2011) In vivo fluorescence imaging of bacteriogenic cyanide in the lung of live mice infected with cystic fibrosis pathogens. PLoS ONE 6, e21387
28. Hong SJ, Yoo J, Kim SH, Kim JS, Yoon J, Lee CH (2009) β-Vinyl substituted calix[4]pyrrole as a selective ratiometric sensor for cyanide anion. Chem Commun 189–191
29. Shiraishi Y, Nakamura M, Yamamoto K, Hirai T (2014) Selective and sensitive fluorometric detection of cyanide anions in aqueous media by cyanine dyes with indolium–coumarin linkages. Chem Commun 50:11583–11586
30. Shiraishi Y, Sumiya S, Manabe K, Hirai T (2011) Thermoresponsive copolymer containing a coumarin–spiropyran conjugate: reusable fluorescent sensor for cyanide anion detection in water. Appl Mater Interfaces 3:4649–4656
31. Shiraishi Y, Adachi K, Itoh M, Hirai T (2009) Spiropyran as a selective, sensitive, and reproducible cyanide anion receptor. Org Lett 11:3482–3485
32. Shiraishi Y, Sumiya S, Hirai T (2011) Highly sensitive cyanide anion detection with a coumarin–spiropyran conjugate as a fluorescent receptor. Chem Commun 47:4953–4955
33. Chen B, Ding Y, Li X, Zhu W, Hill JP, Ariga K, Xie Y (2013) Steric hindrance-enforced distortion as a general strategy for the design of fluorescence "turn-on" cyanide probes. Chem Commun 49:10136–10138
34. Ding Y, Li T, Zhu W, Xie Y (2012) Highly selective colorimetric sensing of cyanide based on formation of dipyrrin adducts. Org Biomol Chem 10:4201–4207
35. Tang YH, Qu Y, Song Z, He XP, Xie J, Hua J, Chen GR (2012) Discovery of a sensitive Cu(II)-cyanide "off–on" sensor based on new C-glycosyl triazolyl bis-amino acid scaffold. Org Biomol Chem 10:555–560
36. Shi DT, Zhou D, Zang Y, Li J, Chen GR, James TD, He XP, Tian H (2015) Selective fluorogenic imaging of hepatocellular H_2S by a galactosyl azidonaphthalimide probe. Chem Commun 51:3653–3655
37. Lou X, Zhang L, Qin J, Li Z (2008) Analternative approach to develop a highly sensitive and selective chemosensor for the colorimetric sensing of cyanide in water. Chem Commun 44:5848–5850
38. You GR, Park GJ, Lee SA, Choi YW, Kim YS, Lee JJ, Kim C (2014) A single chemosensor for multiple target anions: the simultaneous detection of CN^- and OAc^- in aqueous media. Sensors Actuators B 202:645–655
39. You GR, Park GJ, Lee JJ, Kim C (2015) A colorimetric sensor for the sequential detection of Cu^{2+} and CN^- in fully aqueous media: practical performance of Cu^{2+}. Dalton Trans 44:9120–9129
40. Park GJ, Choi YW, Lee D, Kim C (2014) A simple colorimetric chemosensor bearing a carboxylic acid group with high selectivity for CN^-. Spectrochim Acta A Mol Biomol Spectrosc 132:771–775
41. Lee SA, You GR, Choi YW, Jo HY, Kim AR, Noh I, Kim SJ, Kim Y, Kim C (2014) A new multifunctional Schiff base as a fluorescence sensor for Al^{3+} and a colorimetric sensor for CN^- in aqueous media: an application to bioimaging. Dalton Trans 43:6650–6659
42. Lee HJ, Park SJ, Sin HJ, Na YJ (2015) A selective colorimetric chemosensor with an electron-withdrawing group for multi-analytes CN^- and F^-. Kim, C. New J Chem 39:3900–3907
43. Jo TG, Na YJ, Lee JJ, Lee MM, Lee SY, Kim C (2015) A multifunctional colorimetric chemosensor for cyanide and copper(II) ions. Sensors Actuators B 211:498–506
44. Jo HY, Lee SA, Na YJ, Park GJ, Kim C (2015) A colorimetric Schiff base chemosensor for CN− by naked-eye in aqueous solution. Inorg Chem Commun 54:73–76
45. Song EJ, Kim S, Park GJ, Park SJ, Choi YW, Kim C, Kim J (2014) Selective colorimetric assay of cyanide ions using a thioamide-based probe containing phenol and pyridyl groups. Tetrahedron Lett 55:6965–6968
46. Jo HY, Park GJ, Na YJ, Choi YW, You GR, Kim C (2014) Sequential colorimetric recognition of Cu^{2+} and CN^- by asymmetric coumarin-conjugated naphthol groups in aqueous solution. Dyes Pigments 109:127–134
47. Park GJ, Hwang IH, Song EJ, Kim H, Kim C (2014) A colorimetric and fluorescent sensor for sequential detection of copper ion and cyanide. Tetrahedron 70:2822–2828
48. Tomasulo M, Raymo FM (2005) Colorimetric detection of cyanide with a chromogenic oxazine. Org Lett 7:4633–4636
49. Tomasulo M, Sortino S, White AJP, Raymo FM (2006) Chromogenic oxazines for cyanide detection. J Org Chem 71: 744–753
50. García F, García JM, García-Acosta B, Martínez-Máñez R, Sancenón F, Soto J (2005) Pyrylium-containing polymers as sensory materials for the colorimetric sensing of cyanide in water. Chem Commun 22:2790–2792
51. Ros-Lis JV, Martínez-Máñez R, Soto J (2002) A selective chromogenic reagent for cyanide determination. Chem Commun 19:2248–2249
52. Lee H, Chung YM, Ahn KH (2008) Selective fluorescence sensing of cyanide with an o-(carboxamido) trifluoroacetophenone fused

with a cyano-1,2-diphenylethlene fluorophore. Tetrahedron Lett 49: 5544–5547
53. Miyaji H, Kim DS, Chang BY, Park E, Park SM, Ahn KH (2008) High cooperative ion-pair recognition of potassium cyanide using a heteroditopic ferrocenebased crown ether-trifluoroacetylcarboxanilide receptor. Chem Commun 6:753–755
54. Goswami S, Paul S, Manna A (2013) Carbazole based hemicyanine dye for both "naked eye" and 'NIR' fluorescence detection of CN^- in aqueous solution: from molecules to low cost devices (TLC plate sticks). Dalton Trans 42:10682–10686
55. Goswami S, Manna A, Paul S, Aich K, Das AK, Chakrabotty S (2013) Highly reactive (<1 min) ratiometric probe for selective 'naked-eye' detection of cyanide in aqueous media. Tet Lett 54: 1785–1789
56. Becke AD (1993) Density-functional thermochemistry. III. The role of exact exchange. J Chem Phys 98:5648–5652
57. Lee C, Yang W, Parr RG (1988) Development of the Colle-Salvetti correlation-energy formula into a functional of the electron density. Phys Rev B 37:785–789
58. Hariharan PC, Pople JA (1973) The influence of polarization functions on molecular orbital hydrogenation energies. Theor Chim Acta 28:213–222
59. Francl MM, Petro WJ, Hehre WJ, Binkley JS, Gordon MS, DeFrees DF, Pople JA (1982) Self-consitent molecular orbital methods. XXIII. A polarization-type basis set for second-row elements. J Chem Phys 77:3654–3665
60. Barone V, Cossi M (1998) Quantum calculation of molecular energies and energy gradients in solution by a conductor solvent model. J Phys Chem A 102:1995–2001
61. Cossi M, Barone V (2001) Time-dependent density functional theory for molecules in liquid solutions. J Chem Phys 115:4708–4717
62. O'Boyle NM, Tenderholt AL, Langner KM (2008) Cclib: a library for package-independent computational chemistry algorithms. J Comput Chem 29:839–845
63. Frisch MJ, Trucks GW, Schlegel HB, Scuseria GE, Robb MA, Cheeseman JR, Montgomery Jr JA, Vreven T, Kudin KN, Burant JC, Millam JM, Iyengar SS, Tomasi J, Barone V, Mennucci B, Cossi M, Scalmani G, Rega N, Petersson GA, Nakatsuji H, Hada M, Ehara M, Toyota K, Fukuda R, Hasegawa J, Ishida M, Nakajima T, Honda Y, Kitao O, Nakai H, Klene M, Li X, Knox JE, Hratchian HP, Cross JB, Bakken V, Adamo C, Jaramillo J, Gomperts R, Stratmann RE, Yazyev O, Austin AJ, Cammi R, Pomelli C, Ochterski JW, Ayala PY, Morokuma K, Voth GA, Salvador P, Dannenberg JJ, Zakrzewski VG, Dapprich S, Daniels AD, Strain MC, Farkas O, Malick DK, Rabuck AD, Raghavachari K, Foresman JB, Ortiz JV, Cui Q, Baboul AG, Clifford S, Cioslowski J, Stefanov BB, Liu G, Liashenko A, Piskorz P, Komaromi I, Martin RL, Fox DJ, Keith T, Al-Laham MA, Peng CY, Nanayakkara A, Challacombe M, Gill PMW, Johnson B, Chen W, Wong MW, Gonzalez C, and Pople JA (2004) Gaussian 03, Revision D.01, Gaussian, Inc., Wallingford CT
64. Lee JJ, Park GJ, Choi YW, You GR, Kim YS, Lee SY, Kim C (2015) Detection of multiple analytes (CN^- and F^-) based on a simple pyrazine-derived chemosensor in aqueous solution: experimental and theoretical approaches. Sensors Actuators B 207:123–132
65. Kim HJ, Ko KC, Lee JH, Lee JY, Kim JS (2011) KCN sensor: unique chromogenic and 'turn-on' fluorescent chemodosimeter: rapid response and high selectivity. Chem Commun 47:2886–2888
66. Bergkamp JJ, Decurtins S, Liu S (2015) Current advances in fused tetrathiafulvalene donor–acceptor systems. Chem Soc Rev 44:863–874
67. Pina J, Melo JSD, Breusov D, Scherf U (2013) Donor–acceptor–donor thienyl/bithienyl-benzothiadiazole/quinoxaline model oligomers: experimental and theoretical studies. Phys Chem Chem Phys 15:15204–15213
68. Jia M, Ma X, Yan L, Wang H, Guo Q, Wang X, Wang Y, Zhan X, Xia A (2010) Photophysical properties of intramolecular charge transfer in two newly synthesized tribranched donor−π−acceptor chromophores. J Phys Chem A 114:7345–7352
69. Job P (1928) Formation and stability of inorganic complexes in solution. Ann Chim 9:113–203
70. Tsui YK, Devaraj S, Yen YP (2012) Azo dyes featuring with nitrobenzoxadiazole (NBD) unit: a new selective chromogenic and fluorogenic sensor for cyanide ion. Sensors Actuators B 161: 510–519
71. Noh JY, Hwang IH, Kim H, Song EJ, Km KB, Kim C (2013) Salicylimine-based colorimetric and fluorescent chemosensor for selective detection of cyanide in aueous buffer. Bull Kor Chem Soc 34:1985–1989
72. Na SY, Kim JY, Kim HJ (2013) Colorimetric and fluorometric probe for the highly selective and sensitive detection of cyanide based on coumarinyloxime. Sensors Actuators B 188:1043–1047
73. Park S, Kim HJ (2012) Highly selective chemodosimeter for cyanide based on a doubly activated Michael acceptor type of coumarin thiazole fluorophore. Sensors Actuators B 161:317–321
74. Park S, Kim HJ (2012) Reaction-based chemosensor for the reversible detection of cyanide and cadmium ions. Sensors Actuators B 168:376–380